

See discussions, stats, and author profiles for this publication at: <https://www.researchgate.net/publication/228365681>

Astronomical spectroscopy using an aliased step-and-integrate Fourier transform spectrometer

Article in *Proceedings of SPIE - The International Society for Optical Engineering* · October 2004

DOI: 10.1117/12.552054

CITATIONS

8

READS

41

4 authors, including:



David A. Naylor

University of Lethbridge

305 PUBLICATIONS 4,298 CITATIONS

[SEE PROFILE](#)



Brad Gom

University of Lethbridge

54 PUBLICATIONS 188 CITATIONS

[SEE PROFILE](#)

Some of the authors of this publication are also working on these related projects:



SPICA-Safari [View project](#)



THz Plasmonic Lenses [View project](#)

All content following this page was uploaded by [David A. Naylor](#) on 16 May 2014.

The user has requested enhancement of the downloaded file.

Astronomical spectroscopy using an aliased, step-and-integrate, Fourier transform spectrometer

David A. Naylor^{*a}, Brad G. Gom^a, Margaret K. Tahic^a and Gary R. Davis^b

^aDepartment of Physics, University of Lethbridge, Lethbridge, Alberta, Canada

^bJoint Astronomy Centre, Hilo, Hawaii

ABSTRACT

Fourier Transform Spectrometers (FTS) are commonly operated in a rapid-scan (RS) mode, in which an interferogram of an astronomical source is obtained as quickly as possible, followed by one of a nearby background position. In an alternate operating mode, known as step-and-integrate (SI), the optical path difference in the interferometer is incremented in discrete steps, and the signal is integrated only when the interferometer mirrors are stationary. This mode requires some other means of modulating the signal, such as chopping the secondary mirror so that the detector alternately views source and background. The noise bandwidth in the SI mode (typically ~ 1 Hz) is much smaller than in the RS mode (~ 1 KHz), which in principle can lead to an increase in overall sensitivity. The main problem with the SI mode is that it takes much longer ($\sim 30\times$) to acquire an interferogram. At submillimetre wavelengths, through the use of narrowband optical filters, which are matched to regions of low atmospheric opacity, it is possible to sample the interferogram at less than the interval determined from the DC band limited Nyquist frequency (a condition known as aliasing) and still unambiguously recover the spectral information. We describe in detail the aliased, SI mode of operation of an FTS at the JCMT and present first results of astronomical spectra obtained using this mode. The resulting spectra are compared and contrasted to data obtained in the RS mode.

Keywords: Fourier transform spectroscopy, step-and-integrate, aliased, JCMT, submillimetre

1. INTRODUCTION

Astronomical spectroscopy at submillimetre wavelengths holds much promise for fields as diverse as the early, distant universe to the more recent star formation within our own galaxy. While strong absorption bands of water vapor preclude ground-based observations over much of this spectral range, it is possible to observe in atmospheric *windows*, regions where the earth's atmosphere has partial, though often variable, transmission. Fourier transform spectrometers (FTS), with their inherently broad spectral coverage, intermediate resolution, and intrinsic wavelength and intensity calibration, are particularly well suited to the simultaneous measurement of line and continuum components of source emission.

Since 1990, we have been conducting astronomical observations from the James Clerk Maxwell Telescope (JCMT) using a variety of FTS designs. Initially an existing Michelson interferometer¹, modified to operate at submillimetre wavelengths, was used to measure the atmospheric transmission above Mauna Kea in order to determine the feasibility of conducting broadband spectroscopic observations from the JCMT. These encouraging results provided the impetus for developing a polarizing Martin-Puplett interferometer². The most recent FTS design is based on a Mach-Zehnder configuration³. This design provides access to all four interferometer ports while maintaining a high and uniform efficiency over a broad spectral range. Since the interferometer processes both polarizations, it is twice as efficient as a Martin-Puplett interferometer. Moreover, by using powered mirrors within the arms of the interferometer, the size of the optical beam at the beamsplitter is minimized. Since beamsplitter size is a limiting factor in any FTS, this design is well suited to imaging Fourier transform spectroscopic applications, as evidenced by its selection for the Herschel/SPIRE instrument⁴ and the FTS currently under development for use with the SCUBA-2 camera⁵.

Several noise sources must be considered in Fourier transform spectroscopy. The noise associated with quantum infrared detectors is often dominated by the statistical photon fluctuations of the thermal radiation arising from anything

* naylor@uleth.ca; phone 1-403-329-2426; fax 1-403-329-2057; www.uleth.ca/phy/naylor/

within the detector's field of view. This photon noise has a white noise spectrum (i.e. independent of frequency) and can be minimized by the use of narrow bandpass filters matched to the spectral regions of low atmospheric opacity. Other sources of detector noise include current noise, which has a $1/f$ frequency dependence, and Johnson noise, which again has a white noise spectrum. Additional noise is introduced through the electronics chain (i.e., amplification and digitization), although this can be minimized by careful component selection and cooling of preamplifier resistive networks. At a more subtle level, errors associated with failure to measure accurately the optical retardation of the interferometer mirrors (be it through a misaligned interferometer, poor mirror drive mechanism or errors introduced through the metrology scheme employed) result in distorted spectra whose cause is often difficult to identify. In a practical astronomical application, however, the dominant noise component arises from changes in atmospheric emission and transmission that occur during the acquisition of an interferogram. For example, with typical wind speeds of ~ 30 m/s, the 15 m JCMT views through a different column of air every 0.5 s. In order to minimize the effects of atmospheric variations it is imperative to acquire data as quickly as possible.

2. FTS OPERATING MODES

In Fourier transform spectroscopy, the interferogram signal, $I(z)$, is measured as a function of the optical path difference (OPD), z , between the two arms of the interferometer. While in the ideal world this signal would possess even symmetry, and thus be expressed as the cosine Fourier transform of the incident radiation field, $B(\sigma)$, in practice, wavelength dependent phase is unavoidably introduced and the interferogram takes the form:

$$I(z) = \int_{-\infty}^{+\infty} B(\sigma) \exp(-2\pi i z \sigma) d\sigma$$

Inversion of this equation, duly accounting for the effects of finite optical path, discrete sampling and phase errors, allows the spectrum to be recovered⁶.

Fourier spectrometers can be operated in two modes: rapid scan (RS) and step-and-integrate (SI), briefly discussed below:

2.1 Rapid scan mode

In the *rapid scan* mode, the moving mirror of the interferometer is scanned at constant velocity (typically ~ 1 mm/s), and some form of metrology (e.g., laser, capacitance micrometry, Moiré encoder) is used to sample the interferogram, usually on a uniform OPD grid. In reality, since no translation stage can move at constant velocity, the resulting interferograms will have induced phase errors, although at submillimetre wavelengths and with high quality stages these can often be neglected. When data are obtained on a non-uniform OPD grid, extra processing involving the Fourier transform of irregularly sampled data is required.

In a typical astronomical application employing a single port FTS operating in the RS mode, an interferogram of an astronomical source is immediately followed by one of a nearby background position. However, since interferograms are measured in pairs (corresponding to the up and down scans of the translation stage), and since a pair of full resolution scans takes around a minute, atmospheric stability is likely to be a limiting factor, as will be shown in Sec. 4. When operating with both input ports viewing the sky, an FTS measures the difference between radiation entering each port and thus effectively cancels out variations due to atmospheric emission. However, signal fluctuations due to variations in atmospheric *transmission* during a scan remain and cannot be corrected.

2.2 Step-and-integrate mode

In the *step-and-integrate* mode, the OPD in the interferometer is incremented in discrete steps and the detector signal is integrated when the interferometer mirrors are stationary. The SI mode requires that the translation stage is capable of fast and accurate point-to-point moves. In addition, this mode requires some other means of modulating the signal, such as chopping the secondary mirror, so that the detector alternately views source and background. The modulated signal is detected with a lock-in amplifier. The noise bandwidth in the SI mode is proportional to the reciprocal of the time constant of the lock-in amplifier and is typically around 1 Hz; this is significantly less than the noise bandwidth in the RS mode, which is typically 1 kHz..

The main drawback of the SI mode is that it takes around 30 minutes to acquire an interferogram; this is due to the finite speed of the chopping secondary mirror unit (7.8 Hz for the JCMT), the lock-in time constant (~ 1 s) and the point-to-point motion time of the interferometer stage (~ 0.1 s). In a typical astronomical application employing a single port FTS operating in the SI mode, the difference between the source and background positions is determined by the secondary mirror chop throw (typically 1-2 arcminutes). While the SI mode effectively removes atmospheric emission variations on short timescales, the variation of atmospheric transmission during the long time it takes to complete a high resolution scan remains a problem. The SI mode outperforms the RS mode when extracting the continuum component of emission because this information is encoded around the zero optical path difference region of the interferogram, which is measured, differentially, on much shorter timescales in the SI mode.

3. ALIASED STEP-AND-INTEGRATE MODE

Sensitive submillimetre bolometer detector systems employ narrow-band optical filters to minimize the heat load on the bolometer(s). These filters improve both the overall sensitivity of the detectors and the hold times of the associated low temperature fridges. Moreover, these filters, which are matched to the spectral regions of low atmospheric opacity and possess extremely high out-of-band rejection, confer another advantage which can be exploited by a Fourier spectrometer.

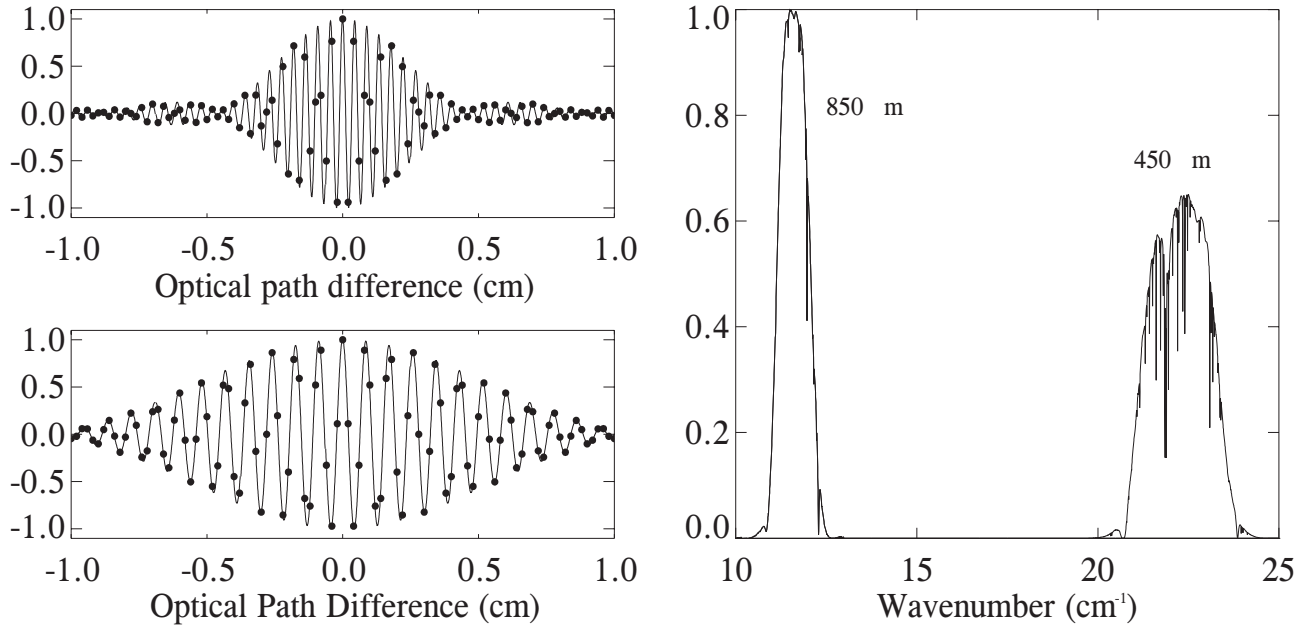


Figure 1. Left: Interferograms for the 450 μm (upper) and 850 μm (lower) bands; symbols represent the DC band limited Nyquist samples corresponding to σ_n of 25 cm^{-1} . Right: The corresponding 450 and 850 μm atmospheric transmission spectra.

From information theory the highest frequency component that can be unambiguously recovered is determined by the Nyquist sampling theorem⁷:

$$\Delta z \leq \frac{1}{2 \cdot \sigma_n}$$

where Δz (cm) is the OPD sampling interval and σ_n is known as the Nyquist frequency (cm^{-1}). Implicit in this relation is the assumption that there are signal components spanning the interval from 0 to σ_n cm^{-1} . Figure 1 shows the interferograms corresponding to the atmospheric transmission at Mauna Kea multiplied by the SCUBA filter characteristics for the 850 and 450 μm bands⁸. Also shown in this figure are the sample points needed to recover these

spectra based on the Nyquist criteria. The sampling is driven by the highest frequency component (i.e., the 450 μm band; $\Delta z = 0.02 \text{ cm OPD}$, $\sigma_n = 25 \text{ cm}^{-1}$).

In the case of a band-limited signal, the minimum OPD sampling interval is given by the Shannon sampling theorem⁹:

$$\Delta z \leq \frac{1}{2 \cdot (\sigma_{\max} - \sigma_{\min})}$$

where σ_{\min} and σ_{\max} are the frequency limits of the signal.

Although the 850 μm filter is narrower and has a lower upper bandpass limit than the 450 μm filter, it is the 450 μm filter that sets the design limit because both signals are sampled simultaneously. Based on the width of the 450 μm filter and the Shannon sampling theorem, the signal bandwidth is $\sim 3 \text{ cm}^{-1}$, which corresponds to a maximum sampling interval of $\sim 0.16 \text{ cm OPD}$. Increasing the sampling interval from that determined by the DC band limited Nyquist frequency case, however, results in aliasing of the spectrum. Since the FTS observes both the 850 and 450 μm bands simultaneously, the challenge is to find an optical path sampling interval that will alias both bands such that neither loses spectral integrity.

Figure 2 shows one possible solution; by choosing a sampling interval of $\Delta z = 0.1 \text{ cm OPD}$, corresponding to a Nyquist frequency of 5 cm^{-1} , it can be seen that spectra from both bands can be retrieved with integrity. This technique provides at least a factor of five reduction in the required sampling rate over a DC band limited measurement, which translates to a factor of 5 decrease in scan time for the aliased step-and-integrate mode. This is only possible due to the high out-of-band rejection of the SCUBA filters.

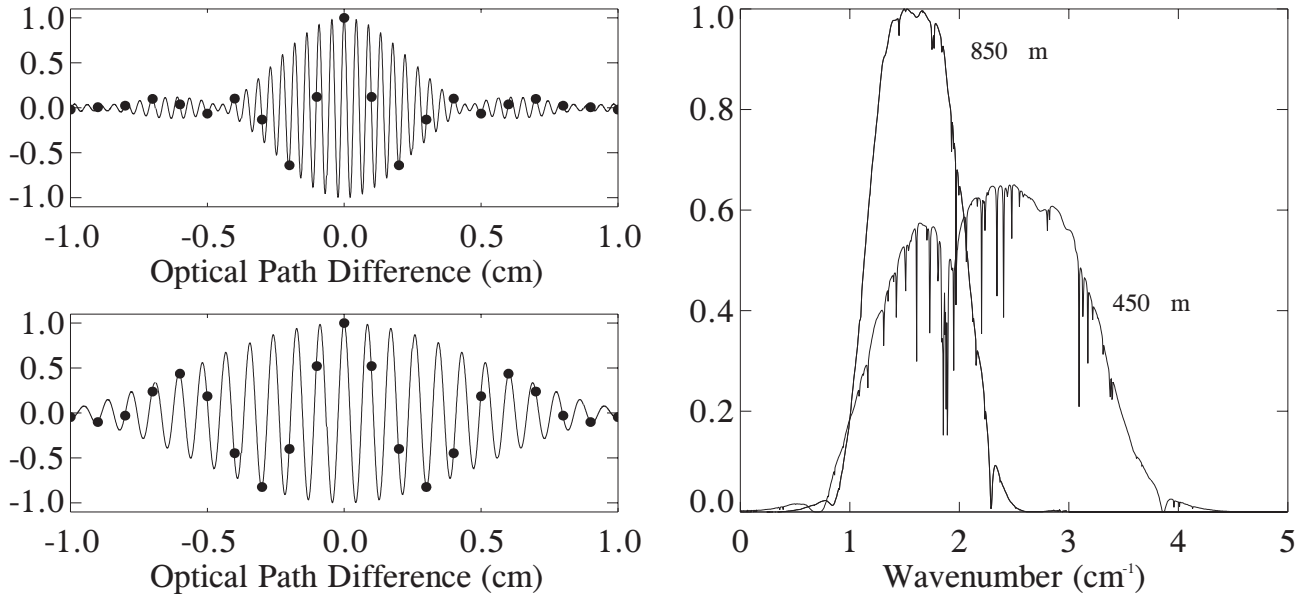


Figure 2. Left: Interferograms for the 450 μm (upper) and 850 μm (lower) bands; symbols represent the aliased samples corresponding to σ_n of 5 cm^{-1} . Right: The recovered 450 and 850 μm spectra retain their spectral integrity.

4. RESULTS

The rapid scan and aliased step-and-integrate modes of operation were compared in two observing runs at the JCMT in October 2003 and March 2004. Unfortunately, the weather during both campaigns was of particularly poor quality with the atmosphere containing $\sim 5 \text{ mm}$ precipitable water vapor (pwv). Under such conditions the atmospheric transmission in the 850 μm band is around 35% and the flux from the atmosphere alone is $\sim 8 \times 10^3 \text{ Jy}$ (Figure 3), rendering

astronomical observations all but meaningless. These conditions did, however, provide an ideal worst case in which to test the aliased SI method. Our principal target was the core of the Orion Molecular cloud (OMC1) which has been observed with the JCMT to have a flux of ~ 167 Jy in the $850\ \mu\text{m}$ band¹⁰, or a few percent of the flux from the atmosphere!

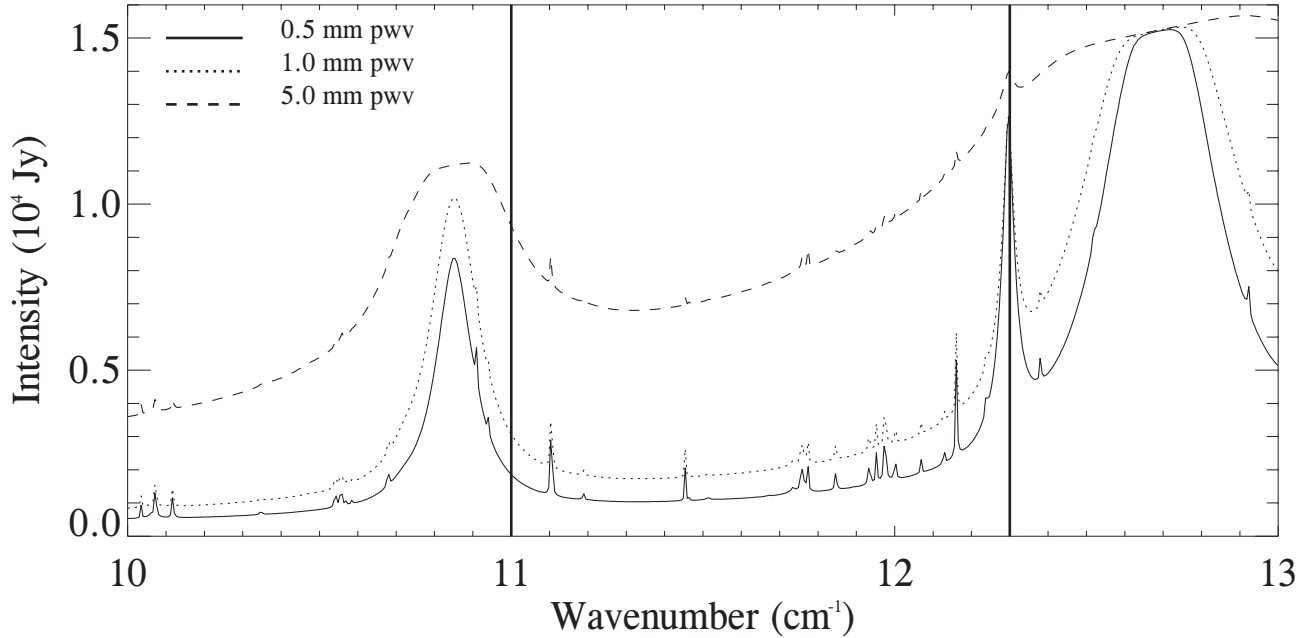


Figure 3. Atmospheric flux (Jy) in the $850\ \mu\text{m}$ window (band edges shown by vertical lines) for varying amounts of precipitable water vapour (0.5, 1 and 5 mm), corresponding to excellent, typical and very poor observing conditions.

4.1 Rapid scan observations

Full spectral resolution scans of OMC1 ($\Delta\sigma = 0.005\ \text{cm}^{-1}$) were obtained in the rapid scan mode. Interferograms were measured in pairs corresponding to up and down scans of the translation stage, each pair taking ~ 140 s. Immediately following, a pair of interferograms was recorded at an adjacent background position chosen to sample the same airmass range observed during measurements of OMC1. Since the atmospheric emission completely dominates the astronomical signal, it is critical to obtain measurements of the source and background as quickly as possible so that the contribution from the atmosphere can be removed. Figure 4 shows single interferograms of the source and background positions, and their simple and phase corrected differences. As expected, the astronomical signal is about a few percent of the total signal.

The interferograms shown in Figure 4 were processed using standard Fourier transform spectroscopy techniques³. Since the optical elements in the FTS and detector produce negligible dispersion over the narrow spectral range of interest, a linear phase correction, determined by weighting phase values obtained from a short double-sided interferogram by the amplitude of the corresponding spectrum, was applied to each interferogram before Fourier transformation. The resulting spectrum is shown in Figure 5 where, in addition to the many spectral lines, a clear continuum component is seen. This continuum component is important because it carries information on the physical properties of the dust in molecular clouds, which plays a key role in the evolution of the interstellar medium.

In total, 12 source-background pairs of RS interferograms were acquired of OMC1, with a total integration time of ~ 30 minutes. As discussed earlier, the weather conditions during these observing runs were extremely poor with over 5 mm pwv along the line-of-sight. Under such conditions, variations of atmospheric emission/transmission at the level of a few percent are common, which completely overwhelm the astronomical signal.

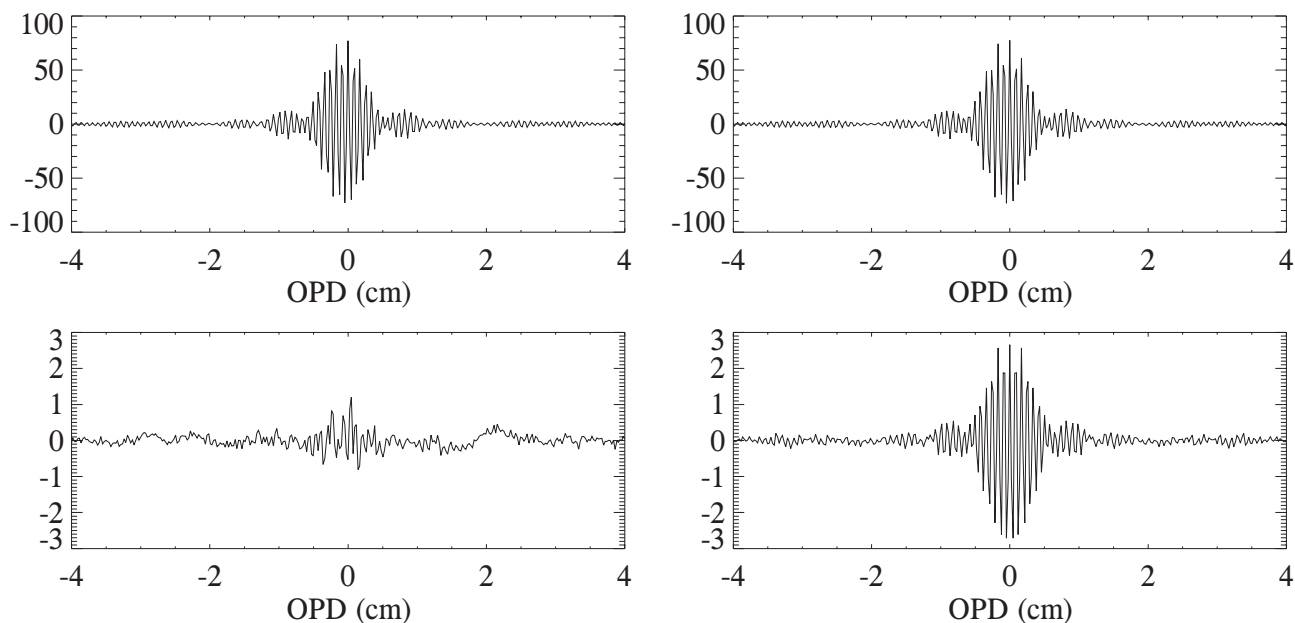


Figure 4. Central region of 850 μm interferograms of OMC1 (top left) and background position (top right); the simple difference between these interferograms, uncorrected for phase errors (bottom left). Difference interferogram when upper two interferograms have been phase corrected prior to subtraction (bottom right). In these figures the abscissa is the optical retardation in cm; the ordinate is arbitrary but of consistent scale.

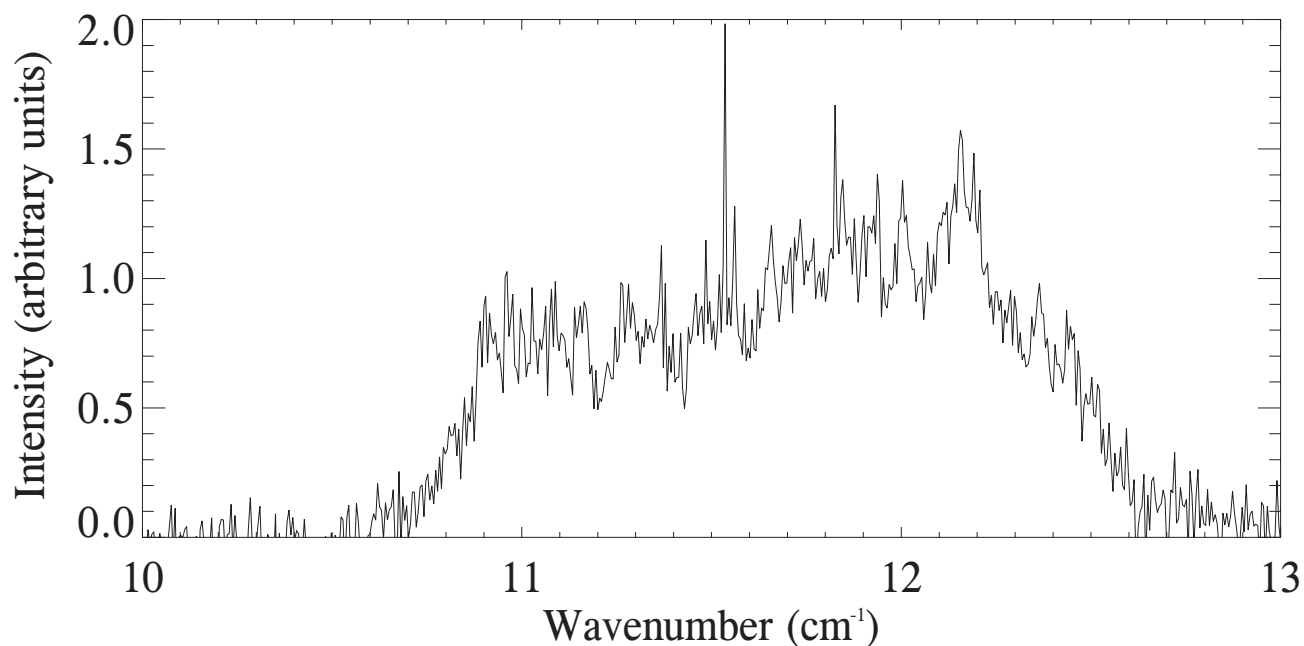


Figure 5. The spectrum obtained from the difference between the Fourier transformation of the top interferograms in Figure 4. Several spectral lines are evident, the largest being the CO J=3-2 transition at 11.53 cm^{-1} . A clear continuum component of emission is seen which provides information on the dust properties of the interstellar medium.

The effects of the varying atmospheric emission/transmission can be readily seen in Figure 6, which shows the 12 difference spectra corresponding to the 12 source-background pairs of RS interferograms. Three of these spectra are

positive, three are negative, and in six cases the continuum flux is effectively cancelled out. It is interesting to note, however, that the CO J=3-2 emission line at 11.53 cm^{-1} can be seen in all spectra. This is to be expected since the continuum information is encoded around the zero optical path difference region of the interferogram, which, in the RS mode, is measured differentially on the timescale of $\sim 140 \text{ s}$ (the atmosphere is rarely stable on such timescales). By comparison the CO line information is encoded throughout the interferogram (because the CO line is unresolved by the FTS) and, since the CO line is not present in the telluric spectrum, its presence in OMC1 is revealed in all 12 difference spectra.

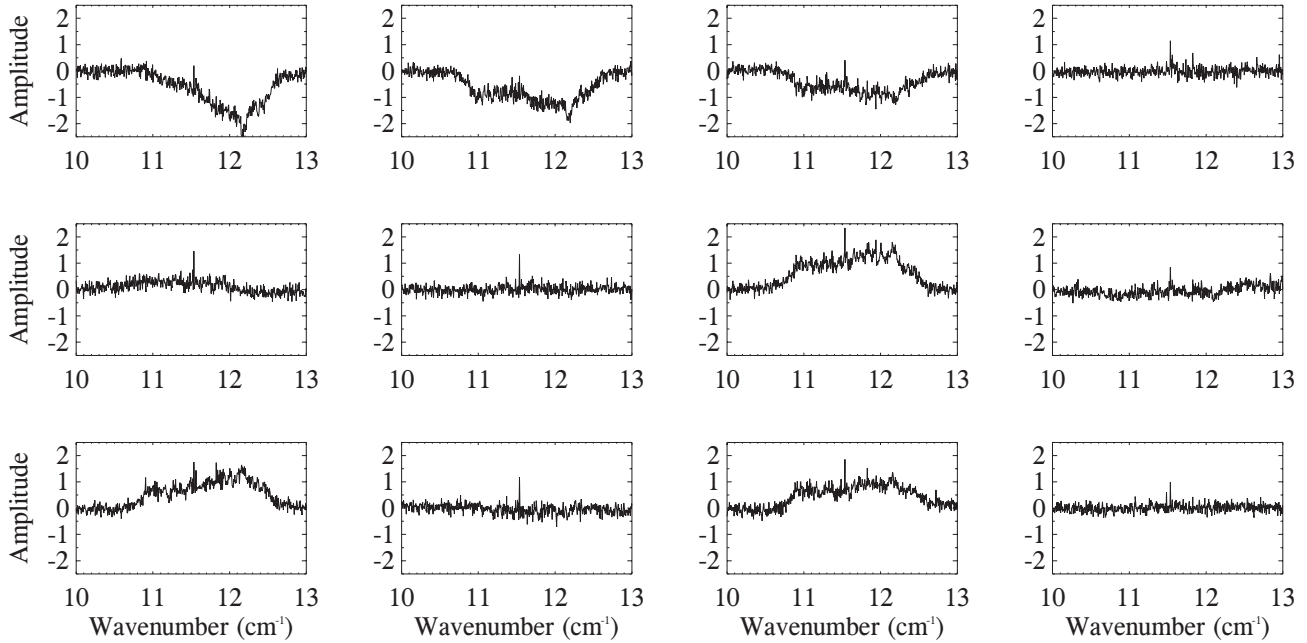


Figure 6. The spectra resulting from the 12 pairs of interferograms discussed in the text. Three of the difference spectra are positive, three are negative and in six cases the continuum flux is effectively cancelled out. In all spectra the CO J=3-2 emission line at 11.53 cm^{-1} can be seen.

4.2 Aliased step-and-integrate observations

A high spectral resolution scan of OMC1 ($\Delta\sigma = 0.005 \text{ cm}^{-1}$) was obtained in the aliased step-and-integrate mode under the same poor atmospheric conditions. The secondary mirror of the JCMT provided the source of modulation for the SI mode, and had a chop throw of $120''$ at a frequency of 7.8 Hz . The FTS drive electronics were modified to move the translation stage of the interferometer in steps of $250 \mu\text{m}$ (corresponding to optical path sampling intervals of 1 mm in the Mach-Zehnder design). The resulting Nyquist frequency of 5 cm^{-1} allows for unambiguous spectral retrieval as was shown in Sec. 3. Following an incremental step, with the translation stage stationary, the modulated detector signal was measured by means of a lock-in amplifier having an integration time constant of 1 s ; the resulting signal was subsequently digitized and stored. The time taken for a full resolution spectrum was ~ 30 minutes; this time could be reduced significantly by having an FTS specifically designed for rapid point-to-point moves and by increasing the modulation frequency.

Standard Fourier transform spectroscopy techniques require phase correction of the interferogram. Phase errors are most commonly introduced by not sampling the interferogram at precisely zero optical path difference. This problem is exacerbated in the aliased mode. Figure 7 shows a theoretical example of the phase error in the undersampled $850 \mu\text{m}$ band. While the sampling error corresponds to a small fraction of a fringe in the continuously sampled interferogram, it has the effect of moving the peak of the undersampled interferogram by more than one fringe. The resulting asymmetry of the sampled interferogram, which yields a complex component in the Fourier transform, and hence phase, is evident.

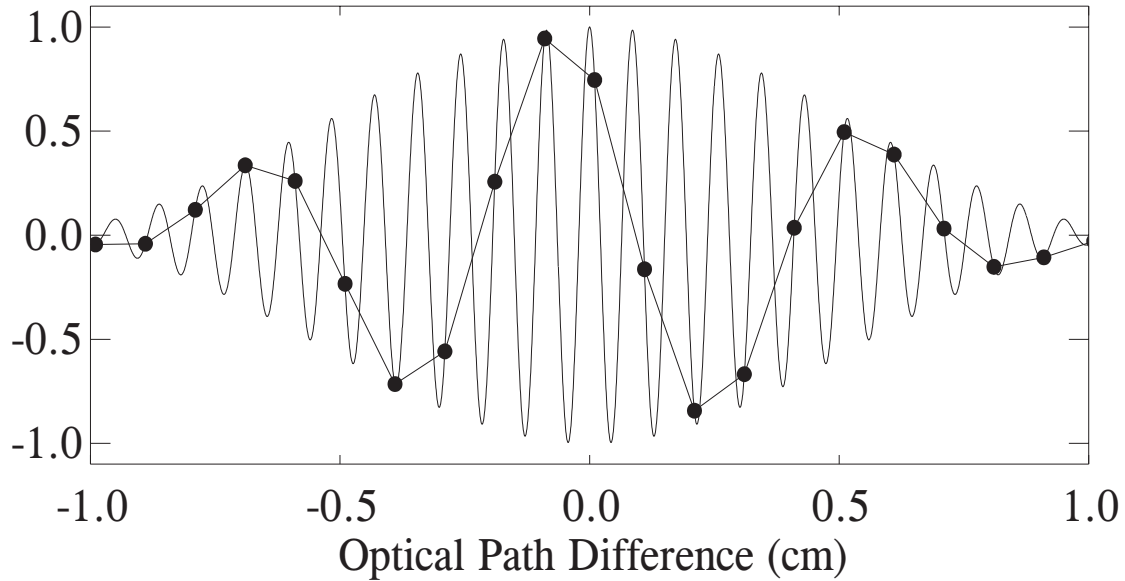


Figure 7. An illustration of how phase errors are introduced into the undersampled interferogram by not sampling precisely at zero optical path difference. The asymmetry of the sampled interferogram (dots) is evident.

The narrowband optical filters, with their high out-of-band rejection, not only allow for the unambiguous recovery of the spectral content when undersampled, but it can also be shown that the undersampled phase information can be recovered by standard processing techniques. Figure 8 shows the slightly asymmetric raw step-and-integrate interferogram (upper panel) and the phase corrected interferogram (lower panel). It can be seen that phase correction has restored the even symmetry of the interferogram.

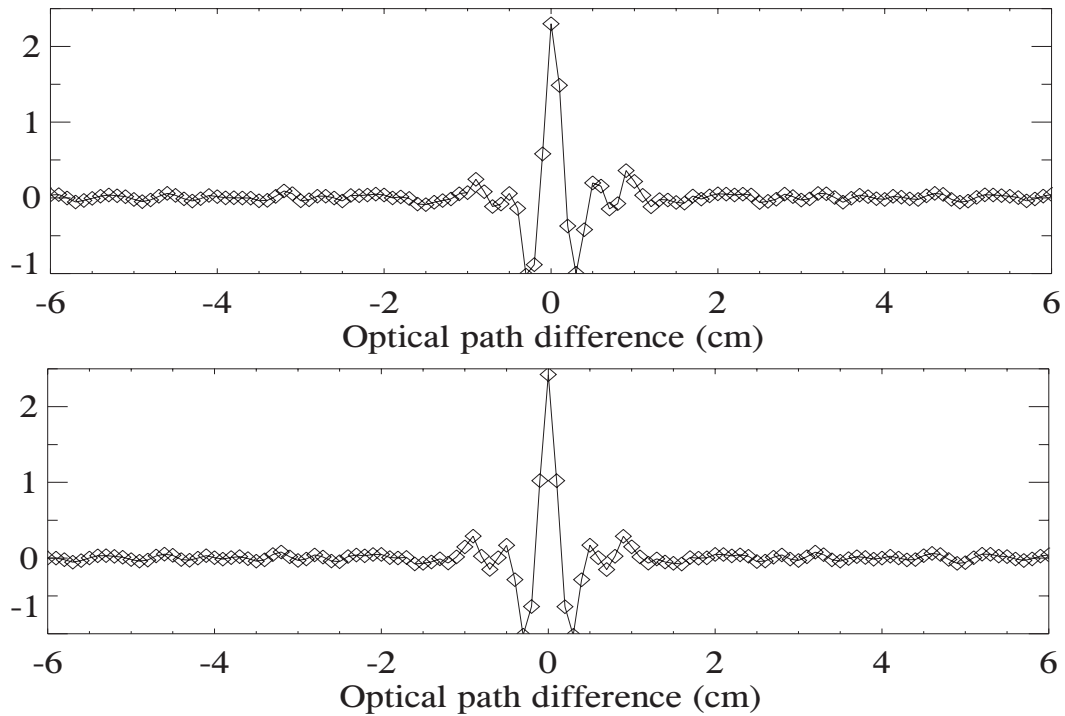


Figure 8. The raw aliased, step-and-integrate interferogram of OMC1 (upper panel) and the corresponding phase corrected interferogram (lower panel).

The spectrum obtained from the Fourier transform of the phase corrected, aliased, step-and-integrate interferogram (lower panel in Figure 8) can be compared with the equivalent spectrum determined from the average of the corresponding rapid scan spectra discussed earlier. The two resulting spectra are compared in Figure 9; it is important to note that the integration time was the same for both the SI and RS observations. Although the observing conditions rendered the quality of these data very poor, it is clear that many spectral lines can still be readily identified in both spectra. The lower trace in the top panel of this figure corresponds to the aliased SI spectrum; the upper trace to the RS spectrum (offset for clarity). Both spectra show a clear continuum component, with the aliased SI spectrum appearing to have better signal-to-noise. In order to quantitatively compare the noise between the two methods it is instructive to look at the signal outside of the bandpass of the optical filter. The lower panel in Figure 9 shows the noise in the 13 to 14 cm^{-1} region for the aliased SI spectrum (upper trace) and corresponding rapid-scan spectrum (lower trace), again offset for clarity. The reduction in noise in the aliased SI mode is evident.

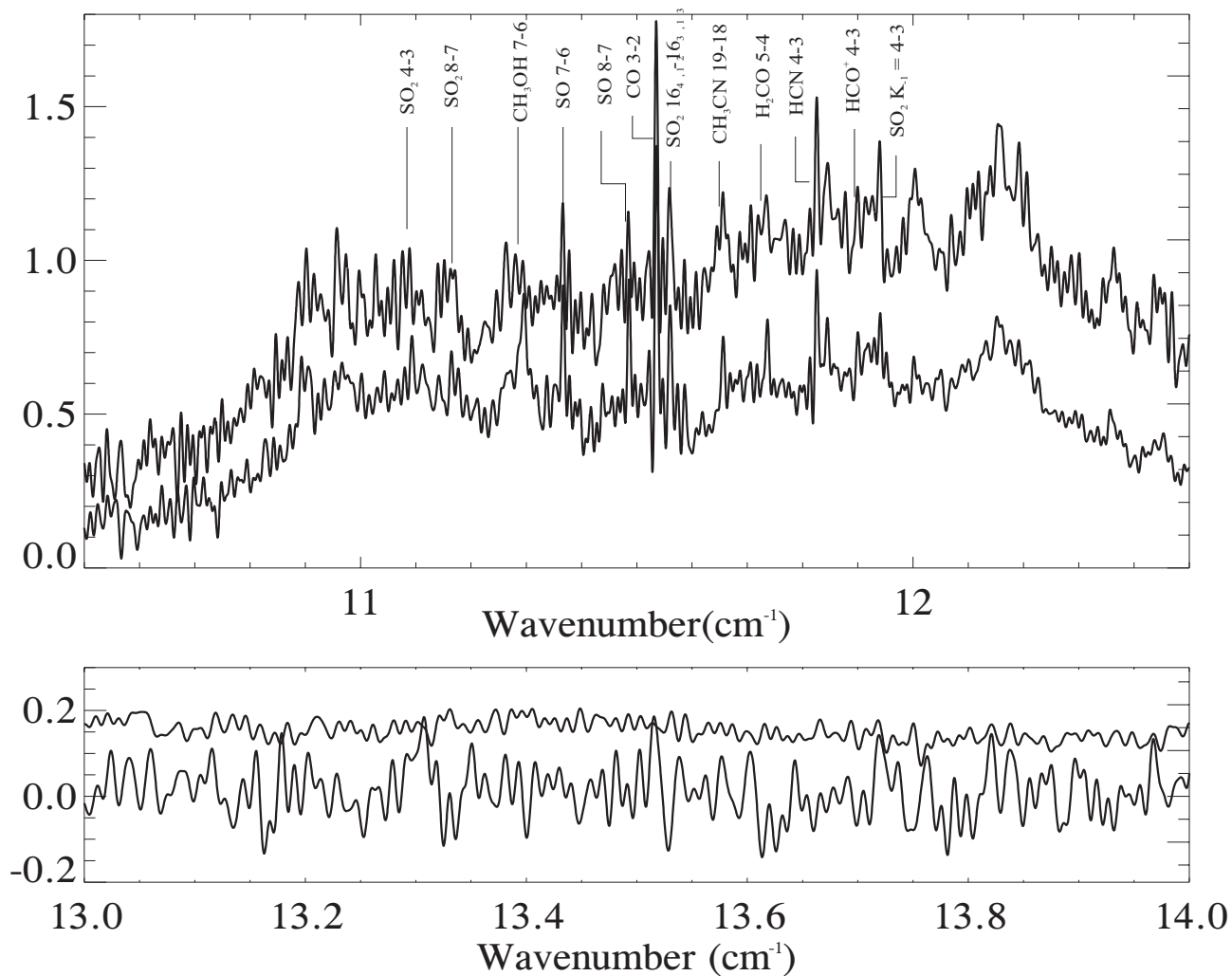


Figure 9. The top panel shows a comparison between the step-and-integrate spectrum of Orion (lower trace) and the corresponding rapid-scan spectrum (upper trace), offset for clarity. The bottom panel shows the out of band noise for the step-and-integrate spectrum (upper trace) and corresponding rapid-scan spectrum (lower trace), again offset for clarity.

5. CONCLUSION

In this paper we have presented the first results from a Fourier transform spectrometer operated in the aliased, step-and-integrate mode. This mode is only made possible through the use of narrowband optical filters, with high out-of-band rejection. Although the observations were conducted under extremely poor atmospheric conditions, a comparison with spectra obtained in the corresponding rapid scan mode in an equivalent time, clearly shows the advantages and potential of this technique. In particular, we have shown the ability of this technique to retrieve the continuum component of emission under varying atmospheric conditions. The aliased SI mode has been shown to outperform the rapid scan mode when it comes to extracting the continuum component of emission (Figure 6) because this information is encoded around the zero optical path difference region of the interferogram, which is measured, differentially, on much shorter timescales. Unfortunately, the spectra obtained to date are of too low quality to warrant detailed astronomical interpretation. We plan to repeat these measurements under, hopefully, better observing conditions in October 2004.

ACKNOWLEDGEMENTS

The authors would like to thank Greg Tompkins and Ian Schofield for modifying the electronics and software, respectively, to accommodate this novel operating mode; Trevor Fulton and Nathan Fitzpatrick assisted with the aliasing analysis. This work would not be possible without the state-of-the-art optical filters provided by Peter Ade's group at Cardiff University. This research is funded in part by grants from NSERC (DAN and GRD). The JCMT is operated by the Observatories, on behalf of the U.K. Particle Physics and Astronomy Research Council, the Netherlands Organisation for Pure Research, and the National Research Council of Canada.

REFERENCES

1. Naylor, D.A. and T.A. Clark, *A mid-infrared astronomical infrared Fourier transform spectrometer*, in Instrumentation in Astronomy VI, Ed Crawford, D.L., Proc. SPIE, **627**, 482—490, 1986.
2. Naylor, D.A., Tompkins, G. J., Clark, T. A. and Davis, G. R., *A polarizing Fourier transform spectrometer at submillimetre and mid-infrared wavelengths*, in Astronomical Telescopes and Instrumentation in the 21st Century, Eds Crawford, D.L and Craine, E.R., Proc. SPIE, **2198**, 703—714, 1994.
3. Naylor, D.A., Gom, B.G., Schofield, I., Tompkins, G., and Davis, G.R., *Mach-Zehnder Fourier transform spectrometer for astronomical spectroscopy at submillimetre wavelengths*, in Millimetre and submillimetre detectors for astronomy, Eds T. Phillips and J. Zmuidzinas, Proc. SPIE, **4855**, 540-551, 2003.
4. Swinyard, B.M., Ade, P.A.R., Griffin, M.J., Dohlen, K., Baluteau, J.-P., Pouliquen, D., Ferand, D., Darfent, P., Michel, G., Martignac, J., Rodriguez, L., Jennings, D., Caldwell, M., Richards, A., Hamilton, P.A. & Naylor, D.A., *The FIRST-SPIRE spectrometer: A Novel Imaging FTS for the Submillimetre*, in UV, Optical and IR Space Telescopes and Instruments, Eds Breckinridge, J.B. & Jakobsen, P., Proc. SPIE, 4013, 196—207, 2000.
5. Gom, B.G., Naylor, D.A., *An update on the imaging Fourier transform spectrometer for SCUBA-2*, Proc. SPIE, **5498**, Millimeter and Submillimeter Detectors for Astronomy II; this volume.
6. Bell, R.J., *Introductory Fourier Transform Spectroscopy*, Academic Press, New York, 1972.
7. Nyquist, H., *Certain topics in telegraph transmission theory*, Trans. AIEE, **47**, 617-644, 1928.
8. Holland, W.S., Robson, E.I., Gear, W.K., Cunningham, C.R., Lightfoot, J.F., Jenness, T., Ivison, R.J., Stevens, J.A., Ade, P.A.R., Griffin, M.J., Duncan, W.D., Murphy, J.A. & Naylor, D.A., *SCUBA: a common-user submillimetre camera operating on the James Clerk Maxwell Telescope*, Monthly Notices of the Royal Astronomical Society, **303**, 659—672, 1999.
9. Shannon, C.E., *Communication in the presence of noise*, Proc. Institute of Radio Engineers, **37**, 10-21, 1949.
10. Johnstone, D. and Bally, J., *JCMT/SCUBA submillimetre wavelength imaging of the integral-shaped filament in Orion*, Ap. J., **510**, L49--53, 1999.